

## Power System Operation Status Based on MRMR Algorithm and Multiple ELM

Ben Kang Jia

CHN ENERGY BENGBU Co., Ltd., Bengbu, 233000, China

### Abstract

To validate the operation status of the power system after encountering faults and restoring it to equilibrium, an efficient and accurate evaluation method is raised to promote the accuracy and efficiency of operation status evaluation model. The study first introduced the minimum redundancy maximum correlation algorithm and multiple extreme learning machine, and then constructed a multi-layer evaluation model grounded on multiple extreme learning machine. The experiment findings indicated that 1225 samples were sent to the second layer after the first evaluation layer, and 531 samples were sent to the third layer after the second evaluation layer. Only 10 samples could not be evaluated at the fifth level. Moreover, there were only 2 cases of missed judgments in the fifth layer. The experiment data indicated that the probability of missed judgments in the hierarchical evaluation model was very small, and it could evaluate almost all samples. This demonstrates that the power system operation state evaluation method based on the minimum redundancy maximum correlation algorithm and multiple extreme learning machine proposed by the research can timely and effectively evaluate feature samples, providing strong support for the stable operation of the power system.

**Keywords:** MRMR, ELM, Power system, Operating status

Received on 09 September 2024, accepted on 12 March 2025, published on 011 June 2025

Copyright © 2025 B. Jia *et al.*, licensed to EAI. This is an open access article distributed under the terms of the [CC BY-NC-SA 4.0](https://creativecommons.org/licenses/by-nc-sa/4.0/), which permits copying, redistributing, remixing, transformation, and building upon the material in any medium so long as the original work is properly cited.

doi: 10.4108/ew.7220

\*Corresponding author. Email: [jbk861008@126.com](mailto:jbk861008@126.com)

### 1. Introduction

With the continuous growth of energy demand and the gradual expansion of power system (PS) scale, the risk of PS interference is increasing. It is significant to evaluate the transient stability of each motor during the transition to a new equilibrium after the PS is disturbed. It is crucial to conduct a comprehensive and accurate evaluation of the power grid on a regular basis, to ensure the safety and stability of this vital infrastructure., ensuring social and economic development as well as safety and stability [1]. However, due to the complexity and variability of the PS, there are still many problems in accurately evaluating its operating status. The commonly used methods for evaluating the operational status of PSs include indicator analysis, trend analysis, and anomaly detection [2-3]. Among them, indicator analysis is to evaluate the operating conditions of the PS by analyzing various indicators of the system. These

indicators can include power load, voltage, frequency, power factor, etc. By monitoring and analyzing these indicators, it is possible to determine whether the operation of the PS is normal and promptly identify problems. Trend analysis is the process of analyzing historical data of the PS to predict future development trends. This can help people develop reasonable operational plans and prepare contingency measures in advance. Anomaly detection is the process of comparing real-time data with historical data to determine if there are any abnormal situations in the system [4-5]. If abnormal situations are discovered, people can take timely measures to eliminate hidden dangers and avoid the problem from escalating. However, these methods suffer from insufficient accuracy and low efficiency in evaluating large-scale systems and complex fault situations.

The accurate assessment of the operational conditions of the PS is of critical importance for guaranteeing its secure and stable operation. Bento MEC proposed a method based on artificial neural networks for calculating load margin in power systems. This method uses synchronous data provided

by phasor measurement units to monitor the load margin of systems that meet voltage stability and small signal stability requirements. The application results indicate that this method is suitable for real-time monitoring of load margin [6]. Aksaeva E and other scholars used trained artificial neural networks to evaluate the operational instability caused by the high penetration rate of renewable energy in the power system. The results show that the network can have a positive impact on the safe and stable operation of the power system [7]. Thomas J. B et al. proposed a new deep convolutional neural network (CNN) transformer model for automatically detecting the type and phase of faults as well as the location of faults in the distribution system, addressing the issues of symmetrical and asymmetrical fault detection. The proposed model utilizes a 1D deep CNN for feature extraction and a transform encoder for sequence learning. The results show that the model has strong detection ability [8]. Yoon D H et al. proposed a deep learning model based on Transformer for real-time diagnosis of power quality disturbances in the power system, which supports end-to-end learning. This study used three-phase voltage and current waveforms from IEEE 9-bus systems as learning sources. The results show that the method is effective for power system diagnosis [9]. Gupta A et al. proposed a scheme based on wavelet transform to enhance the accuracy of fault detection in substations. Simulations were conducted in MATLAB, and the results showed that the method effectively detected faults in substations [10]. Regarding the reliability assessment of PS operation, Hu et al. introduced the concept of Delivered Duty Unpaid (DDU) and proposed an adaptive reliability improvement algorithm. The raised DDU modeling method linked equipment reliability indicators with operational decision variables. The experiment outcomes demonstrated the efficacy of the raised method [11]. Ansari et al. raised a new method for simulating natural gas pipeline failure modes to address the issue of reliability assessment in the operation of power gas networks. This method employed the concept of virtual nodes and adopted a gas release rate model to consider the pinhole, hole, and rupture failure modes of pipelines. Subsequently, the efficacy of the framework was substantiated through its application to three distinct testing systems [12]. Wang put forth a battery inconsistency evaluation model for series-connected battery systems, based on authentic electric vehicle operational data, with the aim of addressing the challenge of assessing the performance of electric vehicle battery PSs. Moreover, an improved robust regression method was used to analyze the evolutionary characteristics of three types of competitive intelligence. The results indicated that this method could effectively evaluate unit inconsistency [13]. Kirilenko et al. analyzed the risks in PS operation using a coherent risk measure to address the uncertainty prediction problem in the PS. Moreover, the origin of risks and their management mechanisms under various sources of uncertainty were elaborated, and an Asymmetric Robust Unit for Risk Avoidance (UR) model for risk avoidance was established. The overall performance of the proposed framework was experimentally validated [14]. Ryu et al. raised a new multi-objective method for

evaluating the success rate of uninterrupted self power supply in microgrids after external power interruption. The method was to optimize the operation planning of Expected Business Continuity Battery Energy Storage System (BESS) in grid connected microgrids. The findings indicated that there are optimal planning results between the operating cost and elasticity of BESS operational planning [15-16].

In summary, domestic and foreign researchers have proposed various evaluation methods for the operation conditions of PSs, including the use of artificial intelligence algorithms. However, few scholars have applied the MRMR algorithm and ELM to assess the operational status of PSs. A PS operation state method based on MRMR algorithm and multiple ELM is proposed to address this issue. The innovation of the research lies in the combination of MRMR algorithm and multiple ELM, fully considering the ability of feature selection and nonlinear processing. At the same time, the hierarchical evaluation model effectively processes large-scale data, raising the accuracy and efficiency of the evaluation model. The results provide technical support for improving the accuracy and efficiency of PS operation status assessment.

## 2. Methods and Materials

As the power grid continues to expand, the losses associated with PS failures are also increasing. To rapidly and accurately assess the operational status of the PS following the occurrence of faults and restore it to a balanced state, a methodology for evaluating the operational status of the PS based on an MR-ELM is proposed. The method first proposes an algorithm for evaluating the operational status of PSs, and then constructs a PS operational status evaluation model based on multiple ELMs.

### 2.1 Algorithm for Evaluating the Operational Status of Power Systems

To quickly and accurately evaluate the operating status of the PS, a combined MRMR algorithm and multiple ELM (MR-ELMs) evaluation algorithm is proposed. The algorithm first extracts feature through MRMR, and then constructs an evaluation model for the operating status of the PS using multiple ELMs. The problem of randomly selecting features during ELM training requires preliminary screening of the PS feature set to ensure that it contains all associated features. The characteristics of PS faults are summarized and classified into power and angle related features. The calculation for equivalent power angle is indicated in equation (1).

$$\delta_{co} = \frac{\sum_{i=1}^N M_i \delta_i}{\sum_{i=1}^N M_i} \quad (1)$$

In equation (1),  $\delta$  represents the equivalent power angle and the center of inertia of  $co$ .  $N$  denotes the

number of generators,  $i$  denotes the generator number, and  $M$  denotes the inertia constant. The calculation of rotor angular velocity is shown in equation (2).

$$\omega_{co} = \frac{\sum_{i=1}^N M_i \omega_i}{\sum_{i=1}^N M_i} \quad (2)$$

In equation (2),  $\omega$  represents the rotor angular velocity. The calculation of angular acceleration is shown in equation (3).

$$\alpha_{co} = \frac{\sum_{i=1}^N M_i \alpha_i}{\sum_{i=1}^N M_i} \quad (3)$$

In equation (3),  $\alpha$  represents the rotor angular velocity. The expression of power related characteristic quantities is shown in equation (4).

$$TZ_1 = \frac{P_{ei}}{P_{mi}} \quad (4)$$

In equation (4),  $TZ_1$  represents the ratio of electromagnetic to mechanical power of the generator,  $P_{ei}$  represents electromagnetic power, and  $P_{mi}$  denotes mechanical power. The average  $TZ_2$  calculation for the electromagnetic to power ratio of all generators is shown in equation (5).

$$TZ_2 = \frac{1}{N} \sum_{i=1}^N \frac{P_{ei}}{P_{mi}} \quad (5)$$

The variance  $TZ_3$  of the ratio of electromagnetic to power for all generators is calculated as shown in equation (6).

$$TZ_3 = \sqrt{\frac{1}{N} \sum_{i=1}^N \left( \frac{P_{ei}}{P_{mi}} - TZ_2 \right)^2} \quad (6)$$

The maximum interference  $TZ_4$  caused by generator failure is calculated as shown in equation (7).

$$TZ_4 = \max(P_{it} - P_{it}) \quad (7)$$

The minimum interference  $TZ_5$  calculation for generator faults is shown in equation (8).

$$TZ_5 = \min(P_{it} - P_{it}) \quad (8)$$

The calculation of rotor kinetic energy  $TZ_6$  is shown in equation (9).

$$TZ_6 = E_i = \frac{1}{2} M_i (\omega_{coi}^2 - 1) \quad (9)$$

In equation (9),  $E_i$  represents kinetic energy. In the angle feature quantity, the power angle variance  $TZ_7$  of all generators is calculated as shown in equation (10).

$$TZ_7 = \sqrt{\frac{1}{N} \sum_{i=1}^N \left( \delta_{coi} - \frac{1}{N} \sum_{j=1}^N \delta_{coi} \right)^2} \quad (10)$$

The angular velocity variance  $TZ_8$  of all generators is calculated as shown in equation (11).

$$TZ_8 = \sqrt{\frac{1}{N} \sum_{i=1}^N \left( \omega_{coi} - \frac{1}{N} \sum_{j=1}^N \omega_{coi} \right)^2} \quad (11)$$

The above feature quantities are an important part of the feature set for PS fault recovery in a stable state. To reduce the subsequent computational workload, it is necessary to conduct more in-depth screening of the feature set. Research introduces the MRMR algorithm for feature extraction to construct the most representative feature set. The MRMR algorithm is a feature selection method that aims to identify a subset of features from the original feature set that exhibit the highest correlation with the target variable and the lowest correlation with one another [17-18]. The fundamental principle of this algorithmic approach is to maximize the degree of correlation between the selected set of features and the target variables while minimizing redundancy within this subset. This ensures that the resulting feature subset possesses both high information content and an avoidance of redundant elements [19-20]. The framework of the algorithm calculation process is shown in Figure 1.

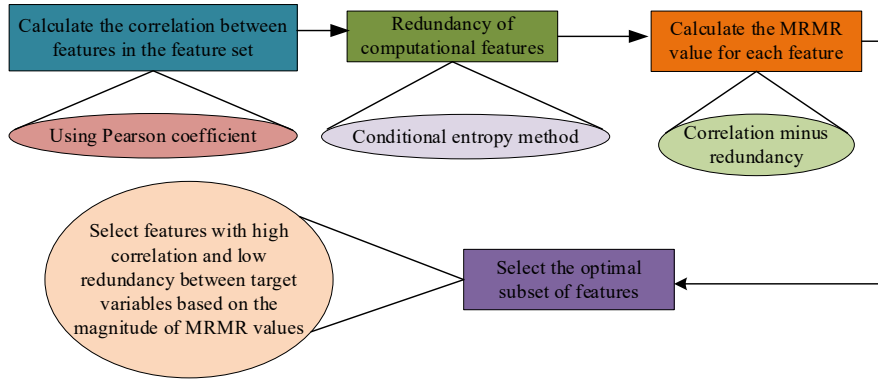


**Figure 1.** MRMR algorithm feature selection calculation framework

In Figure 1, the MRMR algorithm first calculates the correlation between features in the feature set, and then calculates the redundancy of the features. The correlation calculation method can be done through Pearson correlation coefficient, and redundancy calculation can be done through methods such as conditional entropy. After the above steps, it will continue to calculate the MRMR values for each feature. By subtracting redundancy from correlation, the MRMR values of each feature are obtained to determine which features are optimal. Finally, it chooses a subset of features that are highly correlated with the target variable and have low redundancy between them based on the magnitude of the MRMR values. The correlation calculation in the MRMR algorithm is shown in equation (12).

$$U(D, y) = \frac{1}{F} \sum_{i=1}^F MI(f_i, y) \quad (12)$$

In equation (12),  $U$  represents correlation,  $D$  represents dataset, and  $y$  represents target class.  $F$  represents the size of the feature set.  $MI$  indicates mutual information value or similarity, while  $f_i$  represents features.  $MI$  calculation is shown in equation (13).

$$MI(f_i, y) = \sum_{x=1}^s p(f_{i,x}, y_x) \log\left(\frac{p(f_{i,x}, y_x)}{p(f_{i,x})p(y_x)}\right) \quad (13)$$

In equation (13),  $x$  represents the  $x$ th element in the feature,  $S$  represents the total amount of elements, and  $P$  indicates the marginal probability density function. The redundancy calculation in the MRMR algorithm is shown in equation (14).

$$V(F) = \frac{1}{F^2} \sum_{i,j=1}^F MI(f_i, f_j) \quad (14)$$

In equation (14),  $V(F)$  is the minimum redundancy. The mutual information calculation between different features is shown in equation (15).

$$MI(f_i, f_j) = \sum_{x=1}^s p(f_{i,x}, f_{j,y}) \log\left(\frac{p(f_{i,x}, f_{j,y})}{p(f_{i,x})p(f_{j,y})}\right) \quad (15)$$

After completing feature extraction, ELM is applied to construct an operational status evaluation model for the PS. ELM represents an algorithmic approach to single hidden layer feedforward neural networks. In comparison to traditional artificial neural networks, which are known to have limitations such as slow training speeds, susceptibility to local minima, and sensitivity to learning rate selection, the ELM employs a randomized method for establishing connection weights between the input and hidden layers, as well as for determining the thresholds associated with hidden layer neurons. During the training, there is no need to make any adjustments. Only the number of hidden layer neurons needs to be set in order to obtain the optimal solution. Figure 2 illustrates the structure of the ELM network.

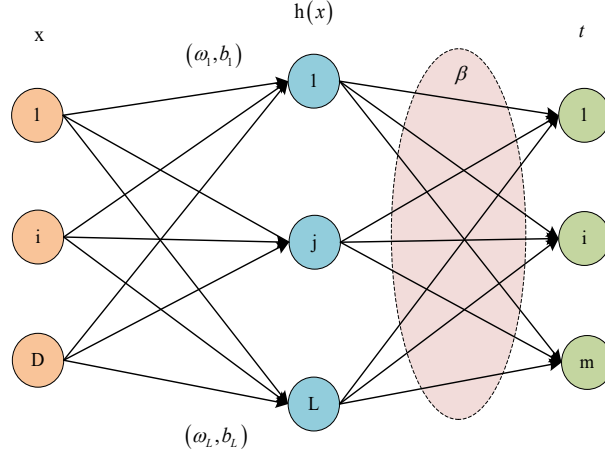


Figure 2. ELM network architecture diagram

In Figure 2, the input of the neural network is the training sample set  $x$ , with a hidden layer in between, and the input layer is fully connected to the hidden layer. The output of the hidden layer is derived by multiplying the input by the corresponding weight and then summing the results of each node through a nonlinear function, which includes the deviation term. The output function of a hidden layer node is not a fixed entity; rather, it can vary depending on the specific output function employed for a given hidden layer neuron. In the figure,  $\omega$ ,  $b$ , and  $\beta$  represent the weights, biases, and output weights on the hidden layer nodes, respectively.  $h$  represents the output of the hidden layer,  $L$  denotes the amount of neurons in the hidden layer,  $i$  and  $j$  denote the  $i$ th and  $j$ th neuron nodes,  $D$  denotes the dataset,  $m$  denotes the amount of nodes in the output layer, and  $t$  is the target value matrix of the training samples. The evaluation of the PS through ELM is divided into two parts. They are offline training and online evaluation, respectively. Offline training mainly obtains simulation data of the PS during operation through fault conditions, aiming to construct models that can be accurately evaluated. Meanwhile, based on the results of offline training, the parameters of the evaluation model can be adjusted to achieve better evaluation performance. Online evaluation can be used for assessing the operational status of PSs. To address the issue that a single ELM cannot fully reflect the characteristics of the PS, multiple ELMs are proposed for parallel evaluation. The multiple ELM training process is shown in Figure 3.

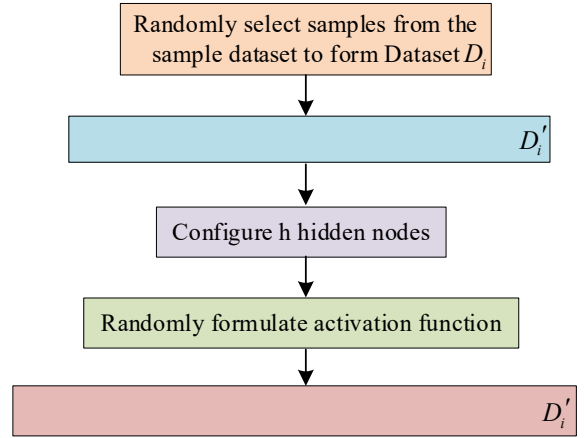


Figure 3. Multiple ELM offline training process

In Figure 3, the offline training process of multiple ELMs involves randomly selecting samples from the sample dataset to form dataset  $D_i$ . Features in  $D_i$  are selected to construct dataset  $D_i'$  and configure hidden nodes. Then it randomly formulates an activation function. Finally, ELM is trained based on the dataset  $D_i'$  and other parameters.

## 2.2 Assessment of Power System Operation Status Based on Multiple Elms

Based on the algorithm proposed above, a PS operation status evaluation model based on multiple ELMs was studied and constructed. The evaluation model was divided into multiple layers based on the number of ELMs and the amount of input information. The flowchart of the PS operation status evaluation method based on multiple ELMs is denoted in Figure 4.

In Figure 4, the first layer of the evaluation model evaluates the working points near the stable boundary of the

system, while the second layer adds more features and ELM to evaluate the working points near the stable boundary. The obtained results determine whether they can be included in the final evaluation. If not, they are sent to the third layer for further evaluation, and so on. If the evaluation result of the final layer cannot be included in the final evaluation, its state

is difficult to estimate and is judged as unstable. The purpose of the first layer in a multi-layer evaluation model is to preliminarily screen feature samples and quickly provide evaluation results. Therefore, the number of selected features and ELMs is half of the final model. The first level evaluation model is denoted in Figure 5.

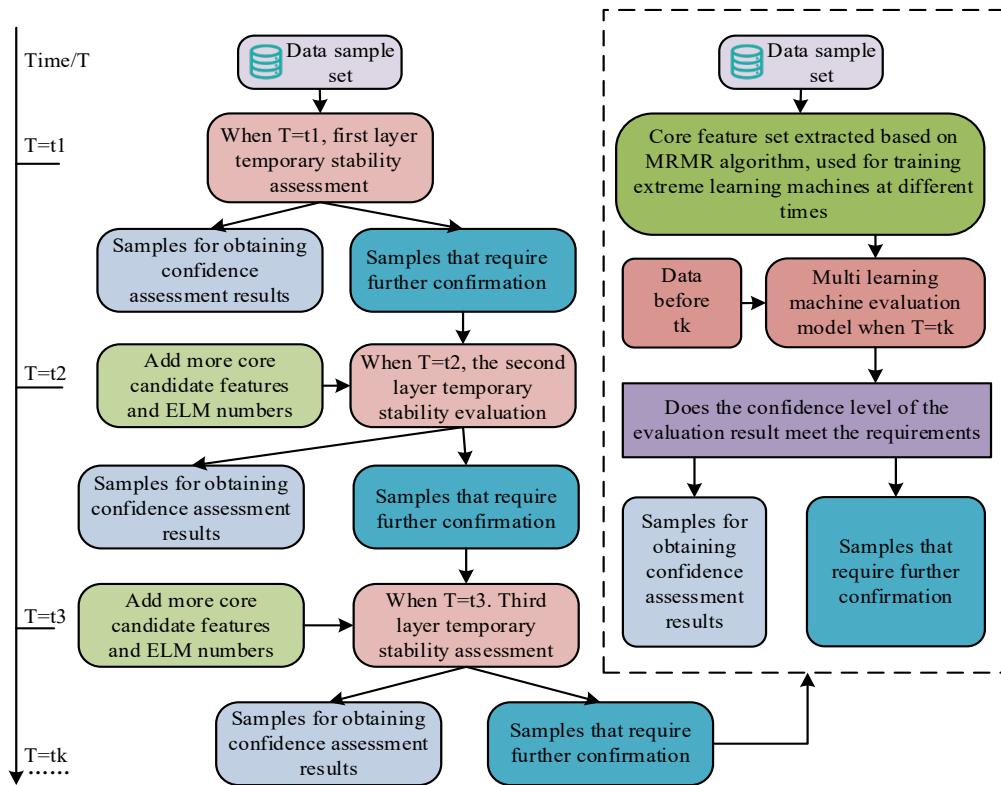


Figure 4. Flow chart of power system operation status evaluation method based on multiple ELMs

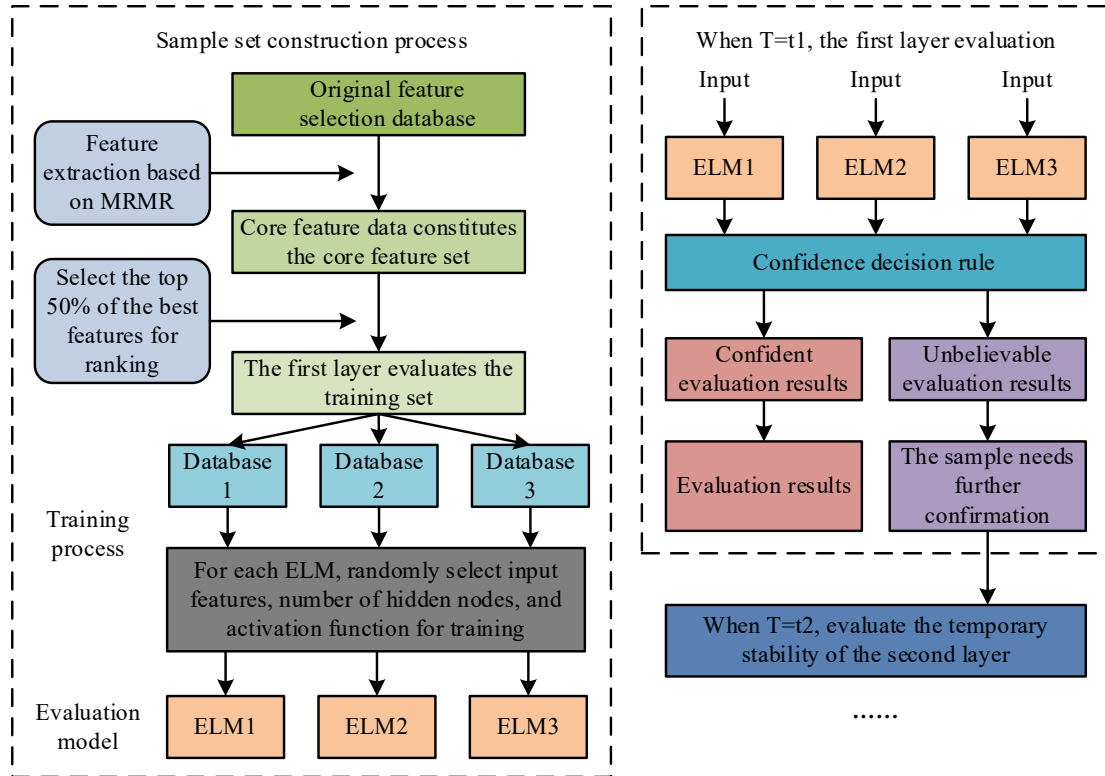


Figure 5. First layer training and evaluation flowchart of multi-layer power system evaluation method model

In Figure 5, the first layer training and evaluation of the multi-layer PS operation status evaluation model is carried out in the following way. The first step is to form an initial feature set and collect key information from the feature set through algorithms to form a key information set. Subsequently, half of the data information in the key feature information set is randomly selected for model training.

Finally, feature information is input into the first layer evaluation model to evaluate it, and judgments are made grounded on the evaluation results. If the evaluation results can be included in the final evaluation, the evaluation ends. If not, it is sent to the next layer for evaluation. The setting of the second layer of the evaluation model is shown in Figure 6.

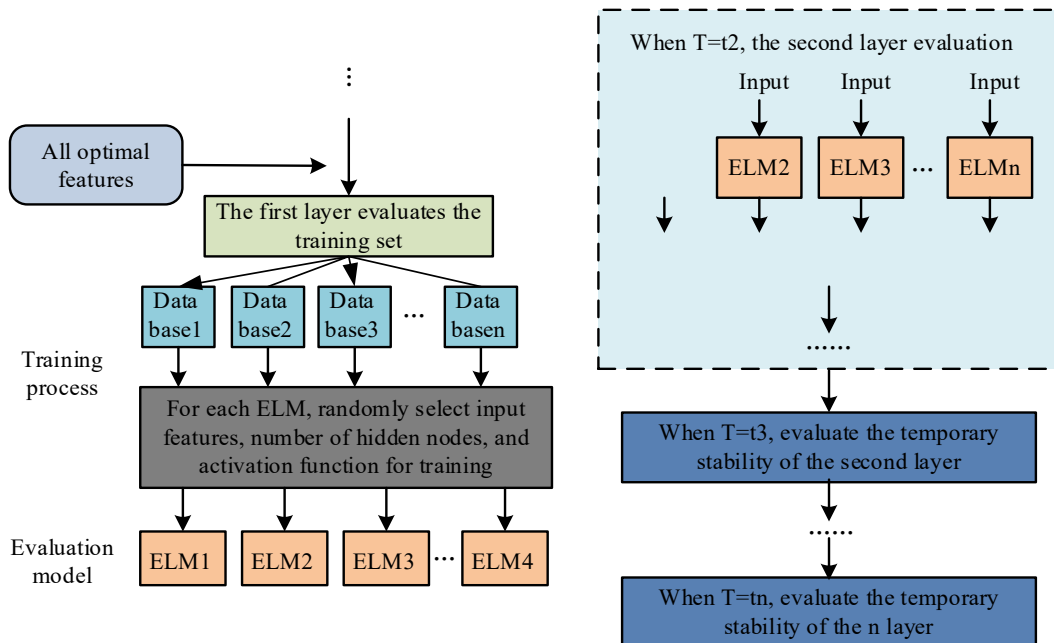


Figure 6. Flow chart for second layer training and evaluation of multi-layer power system evaluation method model

In Figure 6, unlike the first layer, the second layer inputs more information and more complete optimal features, which makes the evaluation accuracy of the second layer higher. Secondly, the second layer adds more ELM compared to the first layer, which helps the model to efficiently utilize information and improve evaluation accuracy. Similarly, samples that cannot be evaluated in the second layer will be sent to the next layer for further evaluation. The subsequent evaluation layers of the model are roughly the same as the first and second layers, and the deeper the layers, the stronger the model's differentiation of samples. If the last layer still cannot partition the samples, to avoid misjudgment, this part of the samples will be judged as unstable.

### 3. Results

To validate the efficacy of the PS operation status evaluation method, MR-ELM, experiments were conducted on the performance of the method in the PS. Firstly, experiments were organized on the impact of different important parameters in the method on the accuracy of model evaluation, and the parameters were adjusted grounded on the experiment outcomes. Subsequently, based on the parameter adjustment results, a case study was conducted on the evaluation model to demonstrate the accuracy of the method in assessing the restoration of the PS to a balanced state after encountering faults.

#### 3.1 Parameter Influence of Power System Operation Status Evaluation Method Based on Multiple ELM

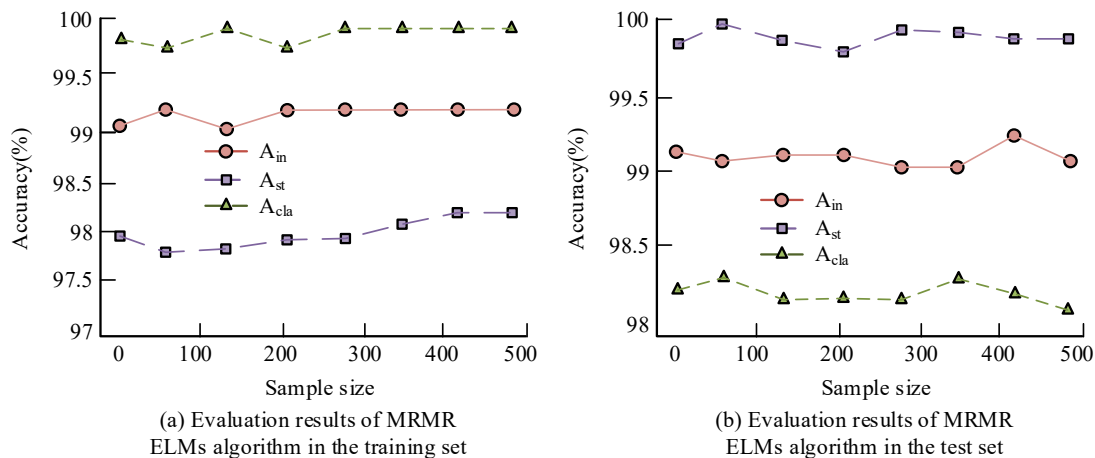


**Figure 7** Evaluation results of MRMR ELMs algorithm on IEEE-39 node system

According to Figure 7 (a), in the training set, the A<sub>in</sub> evaluation index of MRMR-ELMs algorithm was 98.83%, and the A<sub>st</sub> evaluation index of algorithm was 99.88%. The A<sub>cla</sub> evaluation index was 97.98%. Meanwhile, the fluctuation curves of the evaluation accuracy of the three evaluation indicators on the training set were relatively flat

To achieve optimal model performance, the experiment first adjusted several important parameters of the model. Firstly, the IEEE 39 node system was used as the benchmark testing system. Subsequently, based on the characteristics of the selected algorithm and the evaluation purpose, the confidence threshold and ELM quantity were measured. The method was ultimately applied to evaluate the 1648 node system. The parameters of the 1648 node system had a standard deviation  $\sigma$  of 3.33%, and the load varied within 1-1.2 times its initial value. The short-circuit fault was set to a normal distribution in some transformer groups and lines, with a type of three-phase short-circuit, a fault time of  $E$  taken as 0.2s, and a standard deviation taken as 0.014s. There were a total of 13384 fault scenarios, of which 2945 fault types that meet the research direction were selected to be added to the sample set. The basis for evaluating stability was whether the power angle difference of any generator was greater than  $180^\circ$  within 5 seconds after eliminating the fault. The MRMR-ELMs algorithm divided the samples obtained during the IEEE-39 node system evaluation process into a training set and a testing set in an 8:2 ratio. The evaluation of the IEEE-39 node system adopted three indicators: the accuracy of unstable situation classification, the accuracy of stable situation classification, and the overall accuracy of classification, represented by A<sub>in</sub>, A<sub>st</sub>, and A<sub>cla</sub>, respectively. The results of evaluating the IEEE-39 node system using the MRMR-ELMs algorithm are shown in Figure 7.

and the fluctuation amplitude was small. According to Figure 7 (b), in the test set, the A<sub>in</sub> evaluation index was 99.14%, the A<sub>st</sub> evaluation index was 99.97%, and the A<sub>cla</sub> evaluation index was 98.38%. The evaluation accuracy curves of the three evaluation indicators in the test set were similar to those in the training set, and the fluctuation curves

were still relatively small. Experimental data indicated that in the IEEE-39 node system, the MRMR-ELMs algorithm had the highest evaluation among the three indicators, indicating that the algorithm has high evaluation accuracy and strong performance. At the same time, the evaluation accuracy curves in both the training and testing sets were relatively flat with small fluctuations, indicating that the algorithm's performance was relatively stable and reliable. To verify the impact of the amount of selected features and ELM measurement parameters on the effectiveness of the model, a validation experiment was set up. The experiment on the influence of confidence threshold on the model is shown in Figure 8.

In Figure 8 (a), when the confidence threshold was within a relatively strict range (0-80), the confidence level increased from 0 to around 98.5%, and the overall evaluation accuracy  $A_{cla}$  was within the range of 97% to 99%. According to Figure 8 (b), when the confidence threshold was in a relatively loose interval (80-160), the confidence level was around 99.2% to 99.5%. The overall evaluation accuracy  $A_{cla}$  showed a decreasing trend, ranging from 98.2% to 98.5%. According to Figure 8 (c), when the confidence threshold was in the loose interval (160-400), the confidence level increased from 99.5% to 100%, and the overall evaluation accuracy  $A_{cla}$  showed a downward trend, decreasing from 98.2% to 97.4%. Experimental data indicated that when the confidence threshold was in its strictest state, the evaluation accuracy would decrease. When the confidence threshold was relatively loose, the evaluation

accuracy would reach its highest level, and when the confidence threshold was too loose, the evaluation accuracy would also decrease. The confidence threshold was optimal at the intersection of confidence and evaluation accuracy, with an optimal confidence threshold of 80. To investigate the impact of ELM quantity on model evaluation accuracy, evaluation models with different ELM quantities were set up for experiments, and the results are shown in Figure 9.

From Figure 9 (a), in the Group 1 experiments, before the amount of ELMs reached 360, the accuracy of  $A_{in}$ ,  $A_{st}$ , and  $A_{cla}$  increased as the amount of ELMs increased. After the ELM quantity reached 410, the three indicators hardly fluctuated. In Figure 9 (b), in the Group 2 experiment, before the amount of ELMs reached 340, the accuracy of  $A_{in}$ ,  $A_{st}$ , and  $A_{cla}$  increased as the amount of ELMs increased. After the number of ELMs reached 400, the three indicators hardly fluctuated. In Figure 9 (c), in the Group 3 experiment, before the amount of ELMs reached 350, the accuracy of  $A_{in}$ ,  $A_{st}$ , and  $A_{cla}$  increased as the amount of ELMs increased. After the number of ELMs reached 400, the three indicators hardly fluctuated. Based on three sets of experiments, ELM improves the accuracy of the model before reaching a certain number of ELMs, but the risk of overfitting increases after exceeding 400. Therefore, maintaining between 350-400 yields the best model evaluation accuracy. the number of ELMs remained between 350-400, indicating the optimal model evaluation accuracy.

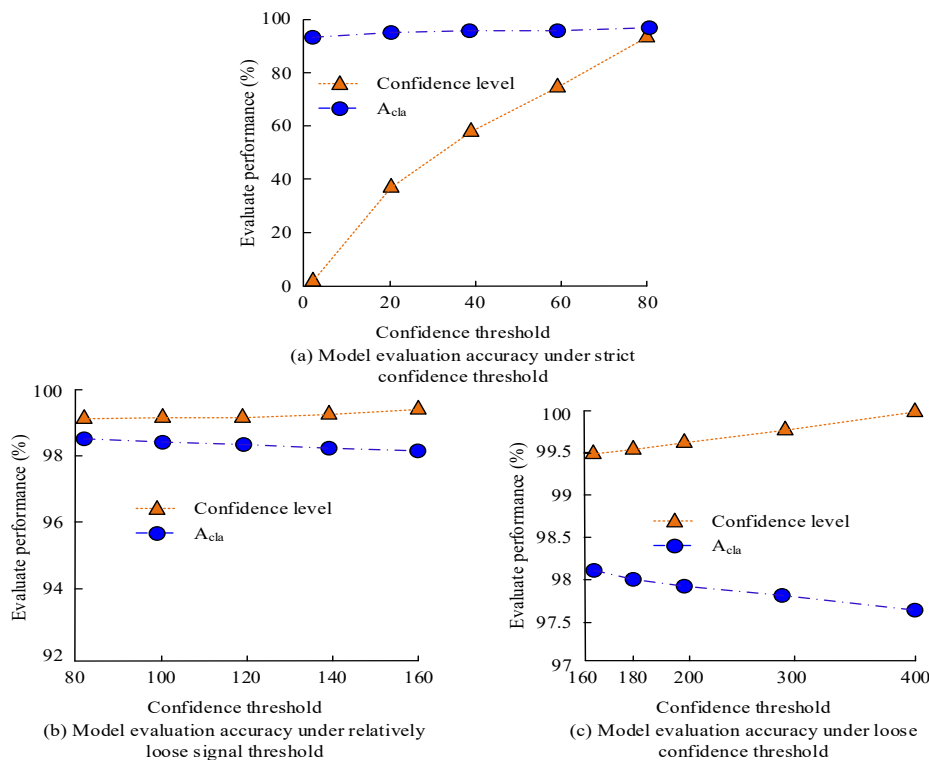
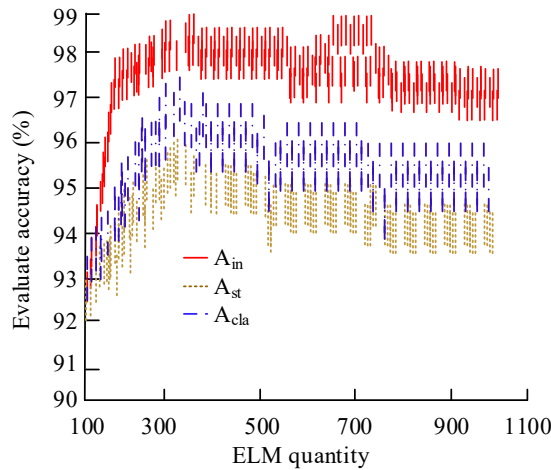
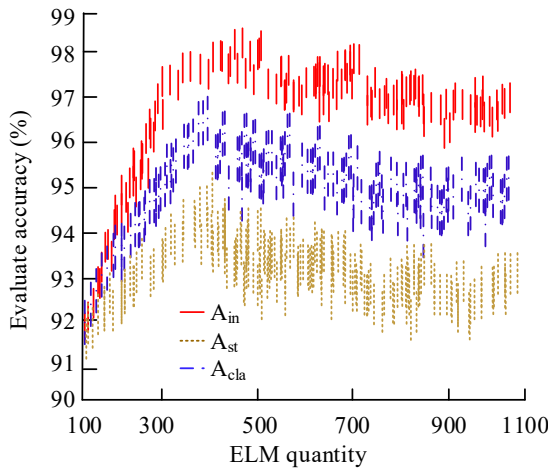


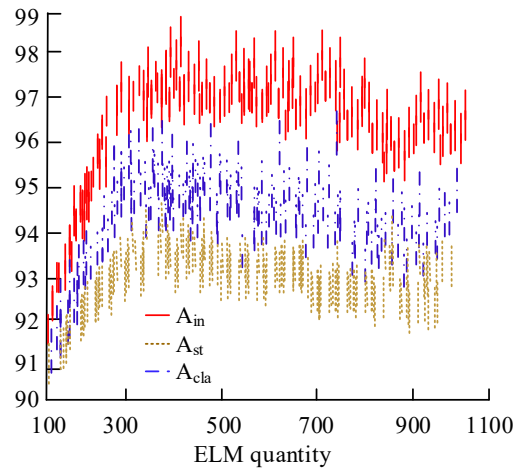
Figure 8. The influence of confidence level and confidence threshold on model evaluation performance



(a) Experiment on the Impact of ELM Quantity on Evaluation Accuracy in Group 1



(b) Experiment on the Effect of ELM Quantity on the Accuracy of Group 2 Evaluation



(c) Experiment on the Effect of ELM Quantity on the Accuracy of Group 2 Evaluation

**Figure 9.** The influence of different ELM numbers on model evaluation accuracy

### 3.2 Analysis of Power System Operation Status Evaluation Based on Multiple Elms

To assess the efficacy of the PS operation status evaluation method based on multiple ELMs, a case study was conducted on a 1648 node system. The parameter settings

were adjusted according to the experiment outcomes mentioned above, and the number of layers in the model was set to 5. The evaluation findings obtained are indicated in Table 1.

Table 1. Evaluation results of the model in the test set

/		Tier 1	Tier 2	Tier 3	Tier 4	Tier 5
Stable sample size	Stable samples	1264	492	266	53	43
	Missing samples	0	0	0	0	2
Unstable sample size	Stable samples	602	217	125	24	28
	Missing samples	11	8	5	72	5
Evaluation time		0.07	0.24	0.36	0.54	0.8
Unbelievable sample size		1225	531	158	72	10

According to Table 1, 1225 samples were sent to the second layer after the first evaluation layer, and 531 samples were sent to the third layer after the second evaluation layer. At the fifth level, 10 samples still could not be evaluated and could not be included in the final evaluation. These 10 samples were considered unstable. Moreover, there were only 2 cases of missed judgments in the fifth layer. The experiment data denoted that the probability of missed

judgments in the hierarchical evaluation model was very small, and it could evaluate almost all samples. This demonstrated that the proposed hierarchical evaluation model could effectively evaluate feature samples. To prove the superior efficacy of the proposed model compared to other evaluation models, a comparative experiment was organized using Support Vector Machine (SVM) and Random Forest (RF). The results are shown in Figure 10.

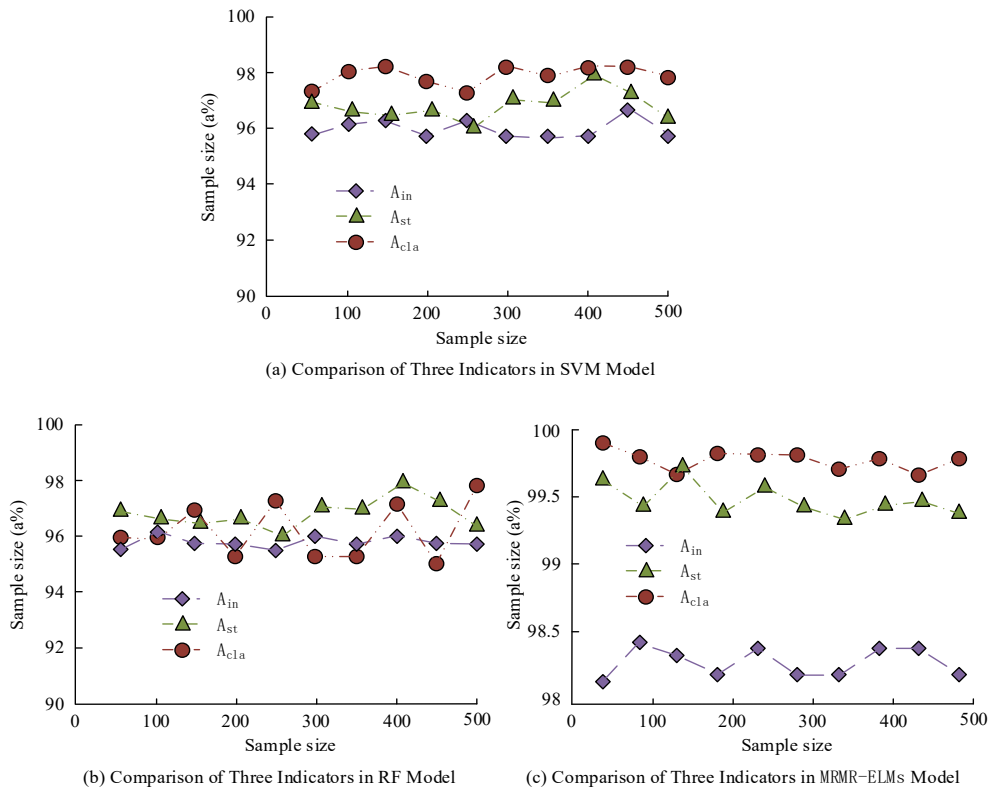
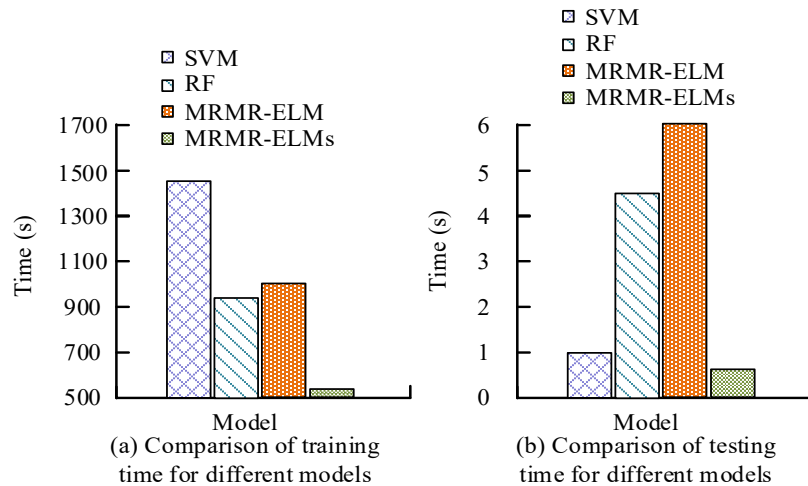


Figure 10. Comparison of evaluation accuracy of different models

According to Figure 10 (a), in the evaluation of SVM, the three indicators of  $A_{in}$ ,  $A_{st}$ , and  $A_{cla}$  were 96.86%, 97.93%, and 98.64%, respectively. In Figure 10 (b), in the evaluation of RF, the three indicators of  $A_{in}$ ,  $A_{st}$ , and  $A_{cla}$  were 96.57%, 97.03%, and 96.86%, respectively. According to Figure 10 (c), in the evaluation of MRMR-ELMs, the three indicators of  $A_{in}$ ,  $A_{st}$ , and  $A_{cla}$  were 98.34%, 99.79%, and 99.89%, respectively. Experimental data showed that the

MRMR-ELMs model proposed by the research had the highest evaluation accuracy, and compared to other algorithms of the same type, MRMR-ELMs had superior performance. To evaluate the processing speed of the MRMR ELMs model, a comparative experiment was conducted using SVM, RF, and MRMR-ELM. The results are shown in Figure 11.



**Figure 11.** Comparison of sample processing speed among different models

According to Figure 11 (a), the training times for SVM, RF, MRMR-ELM, and MRMR-ELMs models were 1484s, 925s, 978s, and 508s, respectively. According to Figure 11 (b), the testing times for SVM, RF, MRMR-ELM, and MRMR-ELMs models were 1 second, 4.5 seconds, 6 seconds, and 0.6 seconds, respectively. Experimental data showed that the MRMR-ELMs model had the least training and testing time, indicating that the MRMR-ELMs model had stronger data processing capabilities compared to other models.

#### 4. Discussion and Conclusion

A method based on MRMR algorithm and multiple ELM was proposed to evaluate the operation status of PS restoration to equilibrium state after encountering faults. The key parameters were adjusted through experiments and the proposed method was validated in the PS. The experiment outcomes denoted that in the training set, the evaluation metrics  $A_{in}$ ,  $A_{st}$ , and  $A_{cla}$  of the MRMR-ELMs algorithm were 98.83%, 99.88%, and 97.98%, respectively. In the test set, they were 99.14%, 99.97%, and 98.38%, respectively. When the confidence threshold was within a relatively strict range, the overall evaluation accuracy  $A_{cla}$  was within the range of 97% -99%. When the interval was relatively loose,  $A_{cla}$  ranged from 98.2% to 98.5%. In the loose interval,  $A_{cla}$  decreased to 97.4%. Before the number of ELMs reached 360, the accuracy of  $A_{in}$ ,  $A_{st}$ , and  $A_{cla}$  increased as the number of ELMs increased. After the ELM quantity reached 410, the three indicators almost no longer fluctuated. In the evaluation of MRMR-ELMs, the three indicators of  $A_{in}$ ,  $A_{st}$ , and  $A_{cla}$  were 98.34%, 99.79%, and 99.89%, respectively. The training time for MRMR-ELMs was 508 seconds, and the testing time was 0.6 seconds. Experimental data illustrated that in the IEEE-39 node system, the MRMR-ELMs algorithm had high evaluations in all three metrics. When the confidence threshold was in its strictest state, the evaluation accuracy would decrease. When the confidence threshold was relatively loose, the evaluation

accuracy would reach its highest level. If the confidence threshold was too loose, the evaluation accuracy would also decrease. The confidence threshold was optimal at the intersection of confidence and evaluation accuracy, with an optimal confidence threshold of 80. The ELM quantity remained between 350 and 400, and the model evaluation accuracy was optimal. The MRMR-ELMs model had the highest evaluation accuracy, and compared to other algorithms of the same type, MRMR-ELMs had superior performance. The MRMR-ELMs model had the least training and testing time, indicating that the MRMR-ELMs model had stronger data processing capabilities compared to other models. In large-scale power systems, due to the complexity and variability of system states, certain states may exhibit many highly nonlinear features. In such a complex feature space, the features of some samples may overlap with those of other samples, making it difficult for the model to correctly determine their state. To address this issue, research will ensure a more balanced ratio of normal and fault state samples during dataset construction. By increasing the sample size under fault conditions, the model can learn the features of different states more comprehensively, improving its ability to identify fault. The model adopts a multi-level evaluation architecture, with each layer conducting in-depth evaluations based on the complexity of input information and sample characteristics. This design allows the model to flexibly adjust the structure of each layer according to changes in the amount of input data, adapting to larger datasets; Using the MRMR algorithm for feature selection enables the model to effectively screen out features that are closely related to the target variable and have low redundancy. When dealing with complex systems, the feature set can be dynamically adjusted according to different input conditions and sample features, which improves the adaptability of the model in changing environments. However, its practical application effect still needs to be verified on more diverse real-world data sources. At present, the data sources used are relatively limited. Future research may consider introducing smart meters, real-time monitoring data, and other related data

sources to further improve the accuracy and adaptability of the model.

## Reference

- [1] Wang J, Lu S, Wang S H, Zhang Y D. A review on extreme learning machine. *Multimedia Tools and Applications*, 2022, 81(29): 41611-41660.
- [2] Rajpal S, Agarwal M, Rajpal A, Lakhyani N., Saggarr A, Kumar N. Cov-elm classifier: an extreme learning machine-based identification of covid-19 using chest x-ray images. *Intelligent Decision Technologies*, 2022, 16(1): 193-203.
- [3] Feng B, Xu Y, Zhang T, Zhang X. Hydrological time series prediction by extreme learning machine and sparrow search algorithm. *Water Supply*, 2022, 22(3): 3143-3157.
- [4] Zhang X, Deng X, Wang P. Double-level locally weighted extreme learning machine for soft sensor modeling of complex nonlinear industrial processes. *IEEE Sensors Journal*, 2020, 21(2): 1897-1905.
- [5] Manoharan J S. Study of variants of extreme learning machine (ELM) brands and its performance measure on classification algorithm. *Journal of Soft Computing Paradigm (JSCP)*, 2021, 3(2): 83-95.
- [6] Bento M E C. Load Margin Assessment of Power Systems Using Artificial Neural Network and Genetic Algorithms. *ifac papersonline*, 2022, 55(1):944-948.
- [7] Aksaeva E, Glazunova A. Artificial Neural Network-based Flexibility Assessment of the Electric Power System with High Wind Energy Penetration. *ifac papersonline*, 2022, 55(9):93-98.
- [8] Thomas J B, Chaudhari S G, Shihabudheen K V, NK Verma. CNN-Based Transformer Model for Fault Detection in Power System Networks. *IEEE Transactions on Instrumentation and Measurement*, 2023(12):72-74.
- [9] Yoon D H, Yoon J. Development of a real-time fault detection method for electric power system via transformer-based deep learning model. *International Journal of Electrical Power and Energy Systems*, 2024, 159(2):22-24.
- [10] Gupta A, Sarangi S, Singh A K. Wavelet Based Enhanced Fault Detection Scheme for A Distribution System Embedded with Electric Vehicle Charging Station. *2023 5th International Conference on Power, Control Embedded Systems (ICPCES)*, 2023(2):1-6.
- [11] Hu B, Pan C, Shao C, Xie, K, Niu T, Li C, Peng L. Decision-dependent uncertainty modeling in power system operational reliability evaluations. *IEEE Transactions on Power Systems*, 2021, 36(6): 5708-5721.
- [12] Ansari O A, Chung C Y, Zio E. A novel framework for the operational reliability evaluation of integrated electric power-gas networks. *IEEE Transactions on Smart Grid*, 2021, 12(5): 3901-3913.
- [13] Wang Q, Wang Z, Zhang L, Liu P, Zhang Z. A novel consistency evaluation method for series-connected battery systems based on real-world operation data. *IEEE Transactions on Transportation Electrification*, 2020, 7(2): 437-451.
- [14] Kirilenko A, Gong Y, Chung C Y. A framework for power system operational planning under uncertainty using coherent risk measures. *IEEE Transactions on Power Systems*, 2021, 36(5): 4376-4386.
- [15] Ryu A, Ishii H, Hayashi Y. Multi-objective optimal operation planning for battery energy storage in a grid-connected micro-grid. *International Journal of Electrical and Electronic Engineering & Telecommunications*, 2020, 9(3): 163-170.
- [16] Kumar A, Bhadu M. A comprehensive study of wide-area controller requirements through real-time evaluation with operational uncertainties in modern power systems. *IETE Journal of Research*, 2023, 69(11): 8382-8403.
- [17] Zhao J, Netto M, Huang Z, Yu S S, Gómez-Expósito A, Wang S, Rouhani A. Roles of dynamic state estimation in power system modeling, monitoring and operation. *IEEE Transactions on Power Systems*, 2020, 36(3): 2462-2472.
- [18] Luo N, Yu H, You Z, et al. Fuzzy logic and neural network-based risk assessment model for import and export enterprises: A review. *Journal of Data Science and Intelligent Systems*, 2023, 1(1): 2-11.
- [19] Chen X, Tang J, Li W, Xie L. Operational reliability and economy evaluation of reusing retired batteries in composite power systems. *International Journal of Energy Research*, 2020, 44(5): 3657-3673.
- [20] Egeland-Eriksen T, Hajizadeh A, Sartori S. Hydrogen-based systems for integration of renewable energy in power systems: Achievements and perspectives. *International journal of hydrogen energy*, 2021, 46(63): 31963-31983.